An improved structural model for cellulose II

James A. Kaduk,[1,a)] and Thomas N. Blanton[2]
[1]*Illinois Institute of Technology, 3101 S. Dearborn Street, Chicago, Illinois 60616*
[2]*Eastman Kodak Company, Kodak Technology Center, Rochester, New York 14650-2106*

(Received 29 December 2012; accepted 5 February 2013)

A sample of cellulose II, prepared by deacetylation of cellulose acetate, has permitted more precise determination of the unit-cell parameters by the Rietveld method. Cellulose II is monoclinic, with space group $P2_1$ *c*-axis unique (or $P112_1$) (No. 4) and refined unit-cell parameters $a = 8.076(13)$, $b = 9.144(10)$, $c = 10.386(20)$ Å, $\gamma = 117.00(8)°$, and $V = 683.5(18)$ Å^3. A density functional geometry optimization using these fixed unit-cell parameters has resulted in an improved structural model for cellulose II. A powder pattern calculated from this new model has been submitted to the ICDD for inclusion in future releases of the Powder Diffraction File. © *2013 International Centre for Diffraction Data*. [doi:10.1017/S0885715613000092]

Key words: cellulose, cellulose II, density functional theory, Rietveld refinement, X-ray diffraction, XRD

I. INTRODUCTION

Cellulose, $(C_6H_{10}O_5)_n$, is a linear macromolecule comprised of β-D-glucose units (Saito, 1989). Cellulose materials are typically semicrystalline (comprised of crystalline and amorphous components), with several crystalline polymorphs known to exist (Fawcett *et al.*, 2013). The generation of cellulose II from native cellulose (cellulose I) can be accomplished using the methods of regeneration (dissolving in a derivative-forming solvent) or mercerization (swelling in concentrated sodium hydroxide) (Kolpak *et al.*, 1978).

A Debye–Scherrer film exhibiting a shriveled and distorted appearance was submitted for analysis. It was determined by X-ray diffraction (XRD) that the polymer film base was cellulose II, an indication that the original film base was cellulose triacetate. Cellulose triacetate can deteriorate with age, characterized by the emission of acetic acid (vinegar syndrome), resulting in a film that becomes brittle, and in extreme cases turns to powder (National Archives, 2000). During this study, cellulose triacetate samples were exposed to various chemical treatments, and some of the resulting samples were identified by XRD as crystalline cellulose II.

The atomic coordinates for cellulose II contained in Powder Diffraction File entry 00-056-1717 (ICDD, 2012) were derived by a density functional geometry optimization (Kaduk and Langan, 2003) of the structure using CASTEP (Milman *et al.*, 2000) and the fixed experimental unit-cell parameters from Langan *et al.* (2001). The preparation of bulk samples of cellulose II mentioned above has permitted the determination of more precise unit-cell parameters, and a new DFT geometry optimization, resulting in an improved cellulose II pattern for the Powder Diffraction File.

II. EXPERIMENTAL

A. Sample preparation

Preparation of cellulose II is based on experiments carried out at Eastman Kodak Company, while studying deacetylation of cellulose acetate-based photographic films. The procedure has been modified so that it can be carried out in a laboratory setting.

Into a glass flask was added 180-g deionized H_2O, 180-g aqueous ammonia (NH_3 assay 29.8%, J.T Baker), and 45-g cellulose acetate powder (Eastman Kodak). Using a magnetic stirrer/hot plate, the mixture was continuously stirred at room temperature for 45 h, then over a period of 1.5 h while heating to 50 °C, and at 50 °C for 3 h. The flask was removed from the hot plate, allowed to cool to 35 °C, stirred for 1 min then filtered (Millipore Type LS) using a vacuum filtration apparatus. The collected solids were washed with 250 ml 40% (v/v) acetic acid/H_2O, followed by two washes with 200-ml glacial acetic acid, and four washes with 250-ml methanol. All solids were transferred to a glass dish and dried at 40 °C for 14 h. An

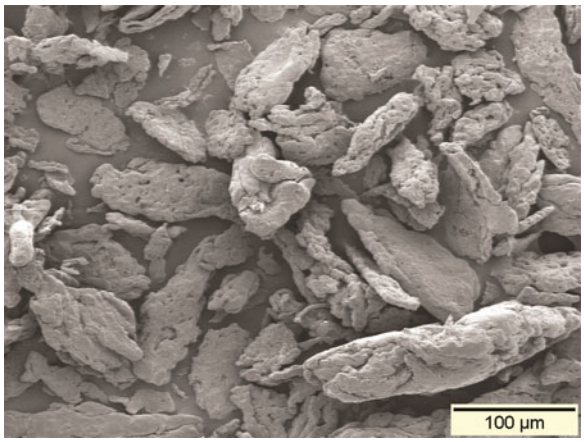

Figure 1. Scanning electron microscope micrograph of cellulose II powder sample.

[a)]Author to whom correspondence should be addressed. Electronic mail: kaduk@polycrystallography.com

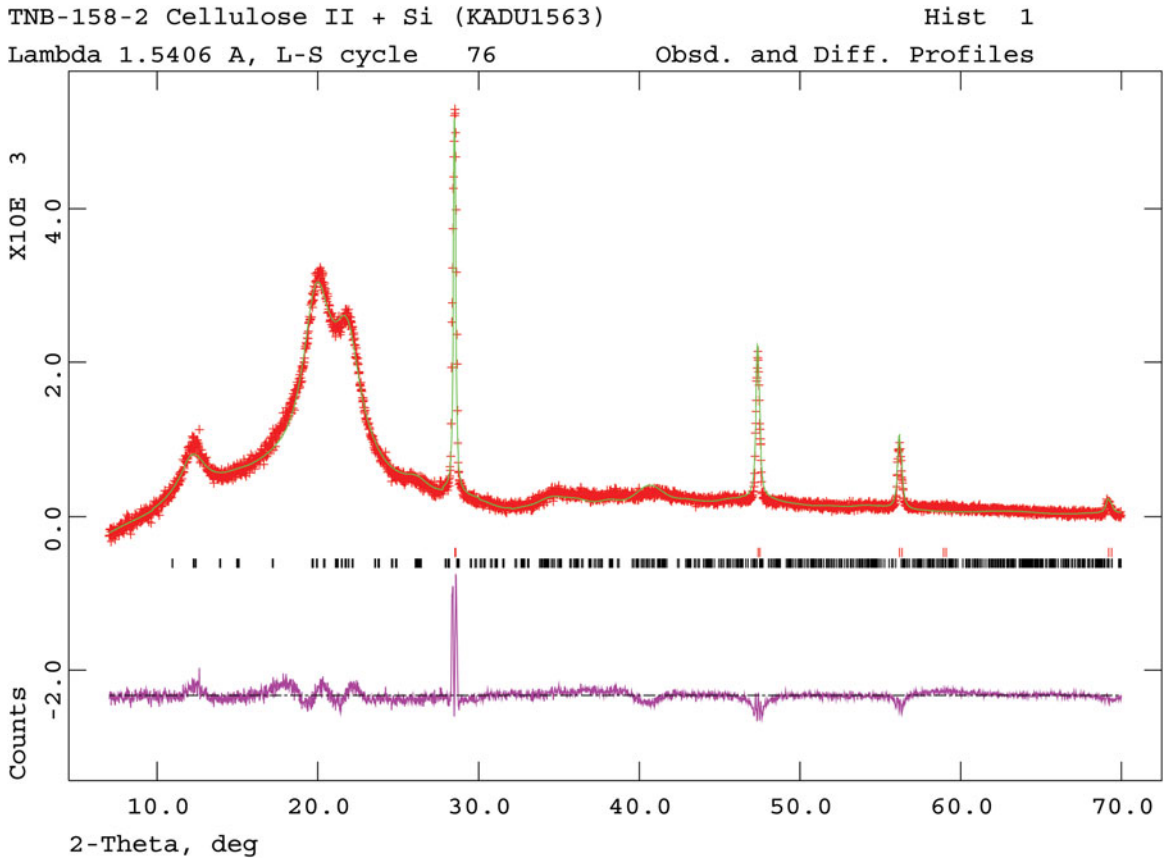

Figure 2. Observed, calculated, and difference patterns from the Rietveld refinement used to determine the lattice parameters of cellulose II. The red crosses represent the observed data points, the green line through them the calculated pattern. The magenta difference curve is plotted at the same vertical scale as the other patterns.

aliquot of the dried powder was analyzed by XRD and identified as cellulose II. A scanning electron microscope micrograph of this cellulose II sample is shown in Figure 1.

B. X-ray diffraction

A portion of the cellulose II sample was blended with ~5 wt% NIST SRM 640b silicon internal standard, and packed into a 50-μm deep quartz zero-background cell. The X-ray powder pattern was measured (5–70°2θ, 0.020 2144° steps, 2 s per step, 0.6-mm divergence slit, 2.5° Soller slits, 1-mm scatter screen height) on a Bruker D2 Phaser diffractometer using only the central 96/192 channels of the LynxEye position-sensitive detector. The resulting XRD pattern was processed by the Rietveld method using GSAS (Larson and Von Dreele, 2004) and the fixed structural model from PDF entry 00-056-1717.

The previous CASTEP (Milman *et al.*, 2000) geometry optimization for cellulose II, used to generate the coordinates in PDF entry 00-056-1717, was carried out using the CGA-PW91 functional, with a plane wave energy cut-off of 340.0 eV (fine basis set), and a *k*-point spacing of 0.08 Å^{-1} (two-point sampling of the Brillouin zone of the primitive cell). The unit-cell parameters were fixed at the experimental values (space group $P112_1$) $a = 8.10(3)$, $b = 9.03(3)$, $c = 10.31(5)$ Å, and $\gamma = 117.10(5)°$. The compound was treated as a metal, and the default number of orbitals was increased by 10% to include some empty orbitals in the calculation. Plausible initial positions for the hydroxyl hydrogen atoms were derived by analysis of the O···O distance of potential hydrogen bonds. The input hydrogen positions were averages of these, in an attempt to avoid local minima.

The Rietveld refinement included phase fractions for cellulose and silicon, as well as cellulose unit-cell parameters. The cellulose profile *X*, silicon profile *Y*, and a common specimen displacement coefficient were refined. The background was modeled using a three-term shifted Chebyshev function; the initial coefficients were based on those obtained from a refinement using data collected at the same conditions on a glucose sample, but the coefficients were refined. A three-term diffuse scattering function was included, with fixed characteristic distances of 1.57(5), 3.15(5), and 8.84(5) Å.

Using the (fixed) refined unit-cell parameters: $a = 8.076(13)$, $b = 9.144(10)$, $c = 10.386(20)$ Å, and $\gamma = 117.00(8)°$, a new geometry optimization was carried out using CRYSTAL09 (Dovesi *et al.*, 2005). The basis sets for the H, C, and O atoms were those of Gatti *et al.* (1994). A density functional calculation using eight *k*-points and the B3LYP functional was carried out.

III. RESULTS AND DISCUSSION

An acceptable Rietveld refinement (Figure 2) was obtained: $R_{wp} = 0.0589$ and $\chi^2 = 4.704$. The transparency of the specimen, even in a thin layer in a zero-background cell, resulted in Si profiles that were hard to describe using GSAS profile function number 2. The refined cellulose profile *X* coefficient of 202(3) corresponds to an average crystallite

https://doi.org/10.1017/S0885715613000092 Published online by Cambridge University Press

TABLE I. DFT optimized atom coordinates for cellulose II, calculated by CRYSTAL09. Space group $P112_1$, $a = 8.076(13)$, $b = 9.144(10)$, $c = 10.386(20)$ Å, $\gamma = 117.00(8)°$, and $V = 683.5(18)$ Å^3.

Atom	x	y	z	U_{iso}, Å^2	Charge
O1	−0.273 59	0.111 94	0.288 18	0.050 00	−0.555
O2	−0.133 51	0.143 24	0.040 58	0.050 00	−0.561
O3	0.028 06	−0.091 55	−0.016 43	0.050 00	−0.535
O4	0.119 24	0.018 90	0.323 63	0.050 00	−0.531
O5	0.247 56	−0.365 06	−0.064 65	0.050 00	−0.589
O6	0.233 13	0.497 24	0.180 34	0.050 00	−0.579
O7	−0.376 04	−0.471 44	0.248 70	0.050 00	−0.535
O8	−0.444 93	0.442 09	−0.09277	0.050 00	−0.527
O9	−0.118 53	0.442 88	−0.079 21	0.050 00	−0.609
O10	0.330 82	−0.143 63	0.309 96	0.050 00	−0.577
C11	−0.052 00	0.014 94	0.363 23	0.050 00	0.384
C12	−0.100 59	0.111 38	0.262 84	0.050 00	0.142
C13	−0.115 04	0.035 02	0.128 87	0.050 00	0.141
C14	0.055 28	0.007 47	0.097 38	0.050 00	0.159
C15	0.100 05	−0.077 44	0.210 07	0.050 00	0.094
C16	0.280 94	−0.09104	0.195 12	0.050 00	0.045
C17	0.467 69	−0.462 98	−0.135 29	0.050 00	0.388
C18	0.321 09	−0.477 56	−0.036 54	0.050 00	0.132
C19	0.393 65	−0.445 13	0.102 73	0.050 00	0.151
C20	−0.481 51	0.471 71	0.131 90	0.050 00	0.162
C21	−0.340 67	−0.492 42	0.023 24	0.050 00	0.101
C22	−0.213 81	0.426 91	0.039 18	0.050 00	0.036
H23	−0.161 08	−0.113 17	0.369 96	0.080 00	0.101
H24	0.012 87	0.236 82	0.260 69	0.080 00	0.125
H25	−0.239 57	−0.084 80	0.129 01	0.080 00	0.088
H26	0.173 75	0.128 20	0.081 13	0.080 00	0.102
H27	−0.015 97	−0.200 85	0.224 48	0.080 00	0.109
H28	0.264 60	−0.173 56	0.114 16	0.080 00	0.115
H29	0.395 07	0.029 89	0.173 03	0.080 00	0.105
H30	−0.427 66	−0.334 19	−0.149 46	0.080 00	0.105
H31	0.208 14	0.396 73	−0.041 51	0.080 00	0.129
H32	0.479 07	−0.311 99	0.114 50	0.080 00	0.111
H33	0.431 97	0.338 38	0.138 43	0.080 00	0.101
H34	−0.255 09	−0.359 34	0.012 25	0.080 00	0.114
H35	−0.114 96	0.485 47	0.117 35	0.080 00	0.120
H36	−0.293 06	0.296 57	0.062 14	0.080 00	0.130
H37	0.266 41	−0.466 23	0.269 33	0.080 00	0.367
H38	0.265 04	−0.332 01	−0.154 99	0.080 00	0.341
H39	−0.296 72	0.098 65	0.379 69	0.08000	0.328
H40	−0.190 19	0.084 00	−0.038 65	0.080 00	0.343
H41	0.014 79	−0.483 03	−0.067 58	0.080 00	0.371
H42	0.236 49	−0.254 85	0.332 54	0.080 00	0.348

size of 39(1) Å. The diffuse scattering function contribution to the pattern is minor. Removing the diffuse scattering function from the refinement yielded a residual ∼18°2θ. Manual integration of this residual suggested the presence of ∼15% amorphous component. Despite the appearance of the pattern, cellulose II is highly crystalline.

The DFT-optimized atom coordinates are reported in Table I. A powder pattern calculated using these coordinates has been submitted to the ICDD for inclusion in future versions of the Powder Diffraction File. The initial and final structures are very similar (Figure 3). The root-mean-square displacement of the non-hydrogen atoms in the C17–C22/O5–O9 monomer at the center of the unit cell is 0.067 Å. The chain–chain differences are larger. The energy difference between the two structures is only 0.12 kcal mole^{-1} of monomer.

As expected, a Mercury/Mogul Geometry Check of the optimized structure (Figure 4) reveals very few geometrical features outside the normal ranges. Only the O3–C11 bond distance of 1.403 Å (1.25(6)) and the O3–C14–C13, C17–C18–C19, O6–C19–C18, and O8–C21–C20 angles of 112.52 (108.0(21)), 113.75 (110.0(19)), 105.09 (110.3(22)), and 106.96° (110.2(16)) fall outside the default Mogul ranges within Mercury. A search directly in Mogul 1.4 (which has larger default tolerances) indicates that the O3–C11 bond is normal [1.395(19) Å], and confirms that the listed angles lie on the tails of the normal distributions in glucose polymers.

The most interesting feature of the structure is the hydrogen bonds (Table II and Figure 5). A positive Mulliken overlap population serves to distinguish real hydrogen bonds from potential (by geometry) hydrogen bonding interactions. The hydrogen bonds involving the methylene side-chain hydroxyl groups O9 and O10 are stronger than the others, but none of the hydrogen bonds are exceptionally strong. Using the correlation that the energy of a hydrogen bond (in kcal/mole) equals $147.1 \times \text{overlap}^{0.53}$ (Kaduk, 2002), these hydrogen bonds contribute 83.5 kcal/mole/monomer to lattice energy.

https://doi.org/10.1017/S0885715613000092 Published online by Cambridge University Press

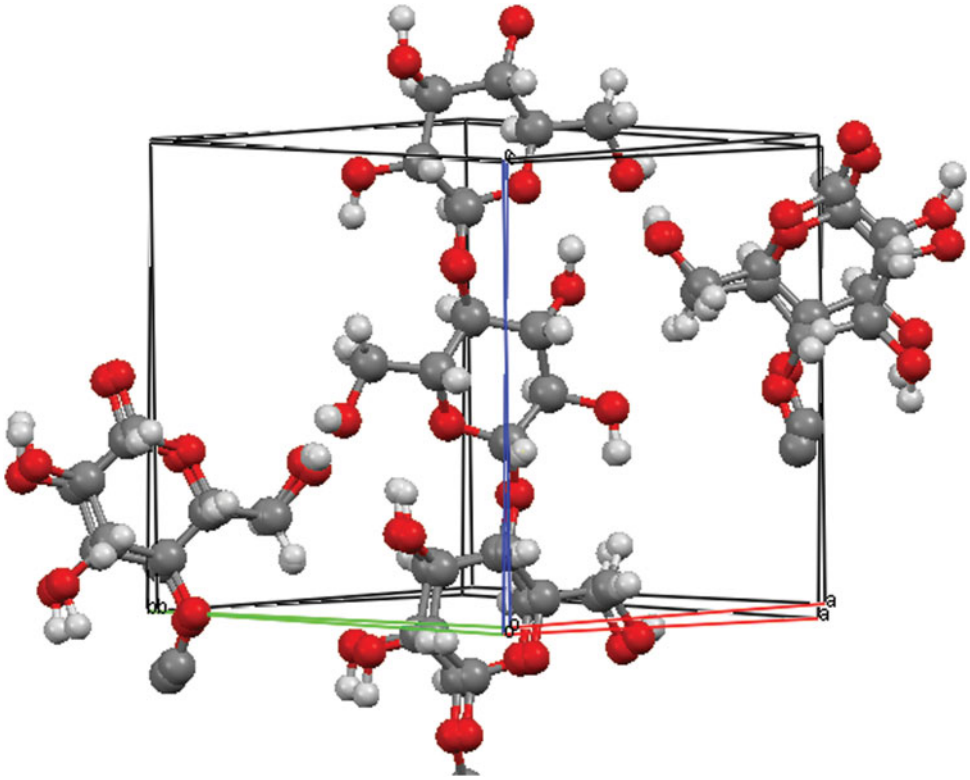

Figure 3. Overlap between the initial (from PDF entry 00-056-1717) and final structural models for cellulose II.

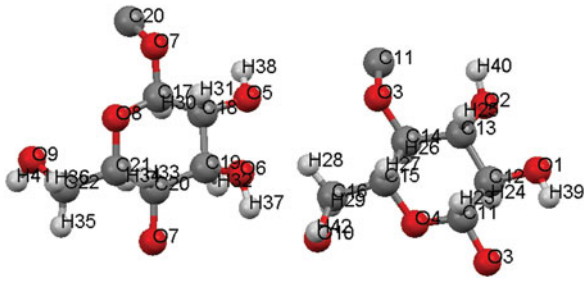

Figure 4. The asymmetric unit of cellulose II, with atom numbering.

The charges on the ether oxygen atoms O3, O4, O7, and O8 are slightly less negative than those on the hydroxyl oxygens. As expected, the hydroxyl hydrogens are more positive than those bonded to carbon. All of the carbon atoms bear a slight positive charge. Any correlation between the charges on the hydrogens involved in the hydrogen bonds and the overlap population is very weak.

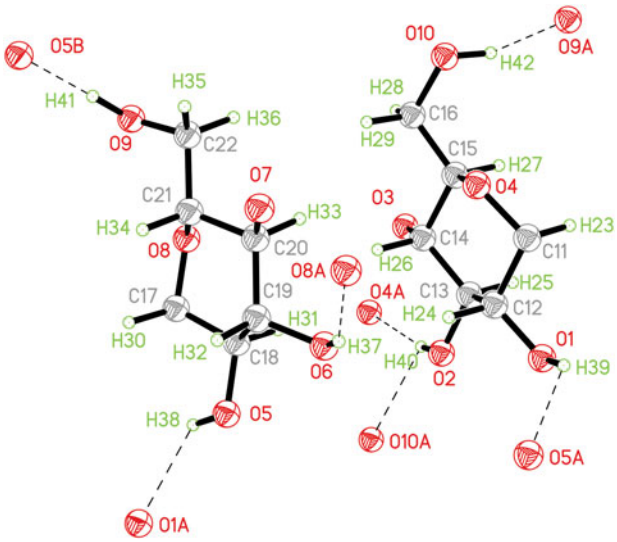

Figure 5. The hydrogen bonds in cellulose II.

TABLE II. Hydrogen bonds in cellulose II.

D–H. . .A	D–H, Å	H. . .A, Å	D. . .A, Å	D–H. . .A, °	Overlap, *e*
O6–H37. . .O8	0.978	1.972	2.815	142.95	0.029
O5–H38. . .O1	0.976	2.068	2.710	120.79	0.037
O1–H39. . .O5	0.966	2.356	2.902	108.28	0.011
O2–H40. . .O4	0.977	1.936	2.728	136.38	0.030
O2–H40. . .O10	0.977	2.150	2.878	130.07	0.038
O9–H41. . .O5	0.985	1.690	2.671	173.07	0.067
O10–H42. . .O9	0.983	1.793	2.737	159.83	0.052

https://doi.org/10.1017/S0885715613000092 Published online by Cambridge University Press

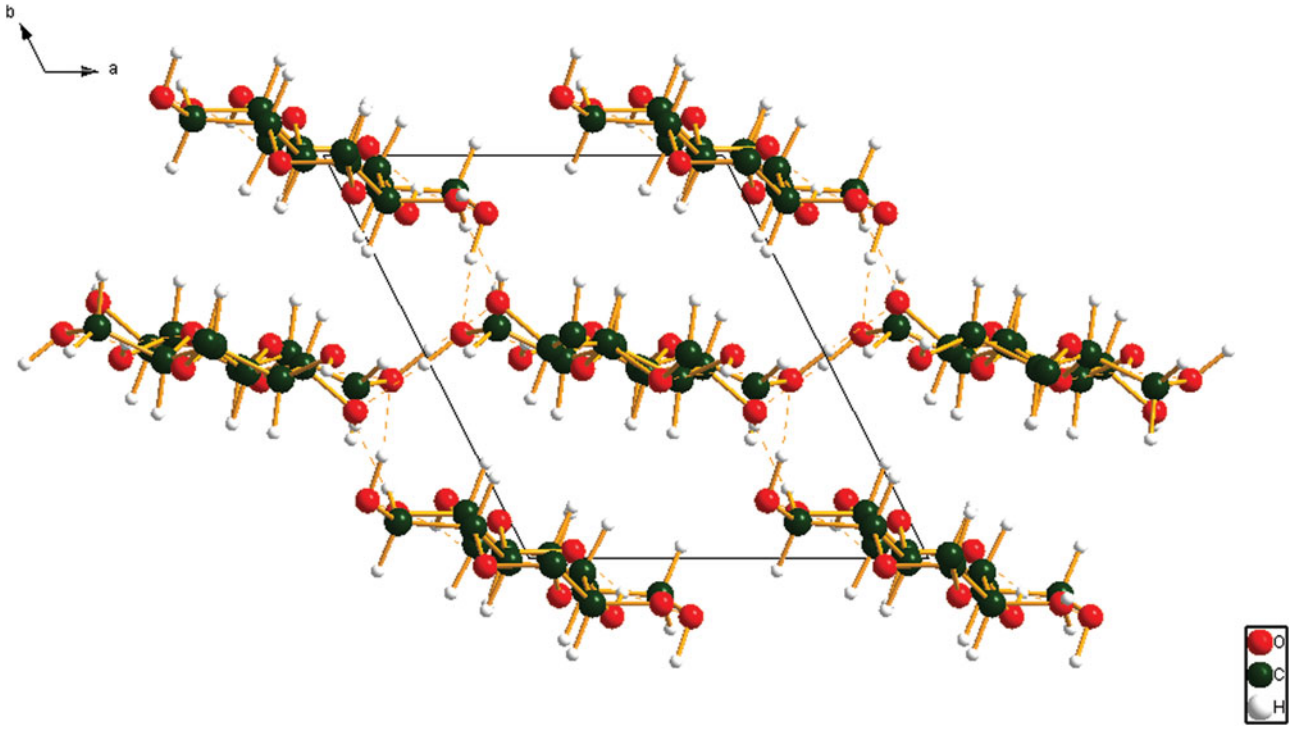

Figure 6. The crystal structure of cellulose II, viewed down the *c*-axis in $P112_1$ (down the chains).

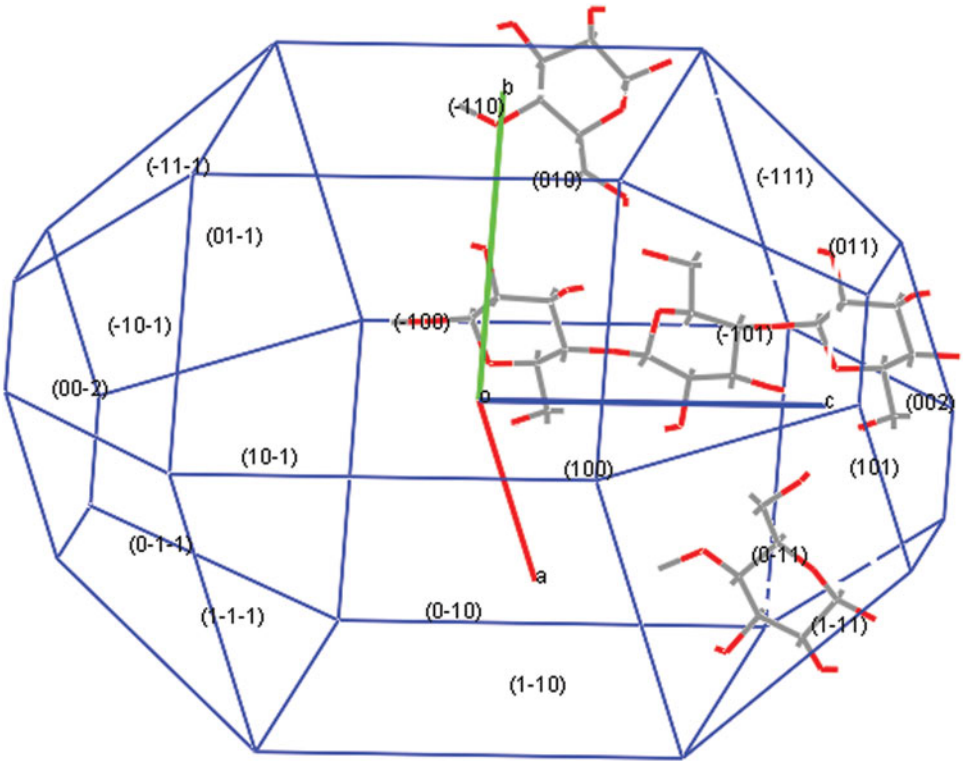

Figure 7. Bravais–Friedel–Donnay–Harker calculated morphology of cellulose II.

There are two crystallographically independent chains in the cellulose II structure (Figure 6), both along the *c*-axis. The planes of the glucose rings lie approximately in the *ac*-plane. The hydrogen bonds involving H38, H39, H41, and H42 link chains, while H37 and H40 participate in intrachain hydrogen bonds. H40 forms bifurcated hydrogen bonds.

The BFDH morphology (Bravais, 1866; Friedel, 1907; Donnay and Harker, 1937; Figure 7) calculated from the crystal structure using Mercury (Sykes *et al.*, 2011), though slightly

https://doi.org/10.1017/S0885715613000092 Published online by Cambridge University Press

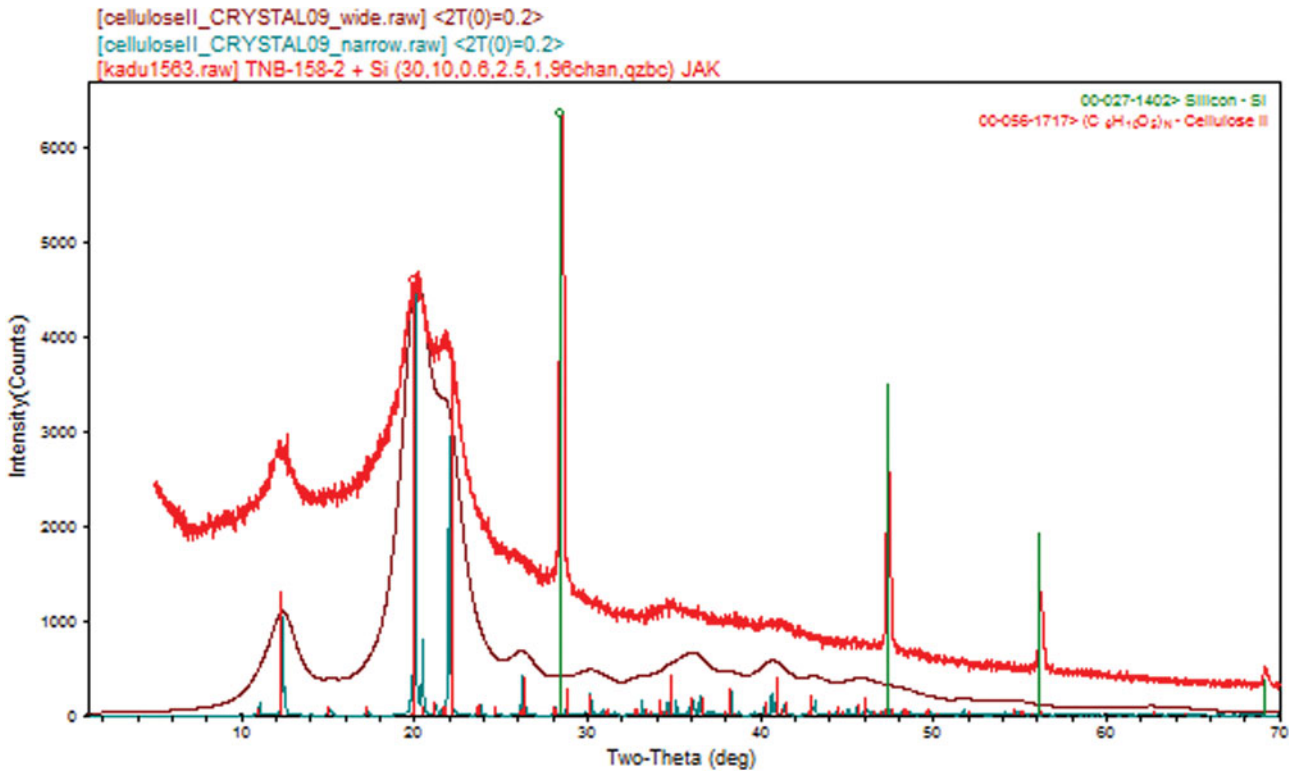

Figure 8. Observed and calculated powder patterns of cellulose II.

elongated along the chain (*c*) axis, is not especially anisotropic. This result suggests that fibers of cellulose II consist of smaller domains. The fibers typically observed in native celluloses (Nishiyama, 2009) are apparently the result of the formation processes rather than the crystal structures themselves.

Powder patterns calculated from this structure model reproduce the observed pattern well (Figure 8). The major deviation is ~34°2θ, a region that is also the poorest in calculated patterns of cellulose I_α and I_β (Fawcett *et al.*, 2013). A pattern based on the one calculated with narrow peaks has been submitted to ICDD for inclusion in future releases of the Powder Diffraction File.

ACKNOWLEDGMENTS

The authors thank Dr Q. Johnson, Materials Data Inc., for providing the distorted Debye–Scherrer film that initiated the study for chemical deacetylation methods for cellulose II generation.

Bravais, A. (**1866**). *Etudes Cristallographiques*, (Gathier Villars, Paris).

Donnay, J. D. H. and Harker, D. (**1937**). "A new law of crystal morphology extending the law of Bravais," Am. Mineral. **22**, 463–467.

Dovesi, R., Orlando, R., Civalleri, B., Roetti, C., Saunders, V. R., and Zicovich-Wilson, C. M. (**2005**). "CRYSTAL: a computational tool for the *ab initio* study of the electronic properties of crystals," Z. Krist. **220**, 571–573.

Fawcett, T. G., Crowder, C. E., Kabekkodu, S. N., Needham, F., Kaduk, J. A., Blanton, T. N., Petkov, V., Bucher, E. and Shpanchenko, R. (**2013**). "Reference Materials for the Study of Polymorphism and Crystallinity in Cellulosics," Powd. Diff **28**(1), 18–31.

Friedel, G. (**1907**). "Etudes sur la loi de Bravais," Bull. Soc. Fr. Mineral. **30**, 326–455.

Gatti, C., Saunders, V. R., and Roetti, C. (**1994**). "Crystal-field effects on the topological properties of the electron-density in molecular crystals – the case of urea," J. Chem. Phys. **101**, 10686–10696.

ICDD (**2012**). PDF-4+ 2012 (Database), edited by Dr. S. Kabekkodu, International Centre for Diffraction Data, Newtown Square, PA, USA.

Kaduk, J. A. (**2002**). "Use of the Inorganic Crystal Structure Database as a problem solving tool," Acta. Cryst. Sect. B: Struct. Sci. **58**, 370–379.

Kaduk, J. A. and Langan, P. (**2003**). "Crystal Structures and Bonding in Cellulose Polymorphs", presented at the 2nd Pharmaceutical Powder X-ray Diffraction Symposium, Concordville PA, 10 December 2002, and at the 52nd Denver X-ray Conference, Denver CO, 4 August 2003.

Kolpak, F. J., Weih, M. and Blackwell, J. (**1978**). "Mercerization of Cellulose: 1. Determination of the Structure of Mercerized Cotton," Polymer **19**, 123–131.

Langan, P., Nishiyama, Y., and Chanzy, H. (**2001**). "X-ray Structure of Mercerized Cellulose II at 1 Å Resolution," Biomacromolecules **2**, 410-416.

Larson, A. C. and Von Dreele, R. B. (**2004**). "General Structure Analysis System, (GSAS)", Los Alamos National Laboratory Report LAUR 86–784.

Milman, V., Winkler, B., White, J. A., Pickard, C. J., Payne, M. C., Akhmatskaya, E. V., and Nobes, R. H. (**2000**). "Electronic Structure, Properties, and Phase Stability of Inorganic Crystals: A Pseudopotential Plane-wave Study," Int. J. Quantum Chem. **77**, 895–910.

National Archives (**2000**). "Managing X-ray Films as Federal Records, National Archives and Records Administration," Office of Records Services, College Park, Maryland, USA, 1-10. Also available at http://www.archives.gov/records-mgmt/publications/managing-xray-films.html.

Nishiyama, Y. (**2009**). "Structure and properties of the cellulose microfibril," Journal of Wood Science **55**(4), 241–249.

Saito, M. (**1989**). "Molecular Characterisation of Cellulose in Aqueous Alkali Solution," in *Cellulose Structural and Functional Aspects*, edited by J. F. Kennedy, G.O. Phillips, and P.A. Williams (Ellis Horwood Ltd., Chichester), pp. 53–80.

Sykes, R. A., McCabe, P., Allen, F. H., Battle, G. M., Bruno, I. J., and Wood, P. A. (**2011**). "New software for statistical analysis of Cambridge Structural Database data," J. Appl. Cryst. **44**, 882–886.

https://doi.org/10.1017/S0885715613000092 Published online by Cambridge University Press